Universidad de Valladolid

Escuela de Doctorado.

TRABAJO FIN DE MASTER

Máster en Física

Mechanics of Elastin-like Recombinamers hydrogels under mechanical wave pressure.

Autor:Alejandro Riol Triviño

Tutor/es: ***José Carlos Rodríguez Cabello.***

Mechanics of Elastin-like Recombinamers hydrogels under mechanical wave pressure.

Author: Alejandro Riol Triviño, José Carlos Rodríguez Cabello.

Date: 24/7/2020

Abstract.

The production of Elastin-like recombiners (ELR) has as objective the production of nano-structural devices that can be used for drug delivery and tissue engineering. The reason of why these materials are so desired are their good mechanical properties, biocompatibility, biodegradability and thermal sensitivity. The objective of this master thesis is to measure the propagation of mechanical waves inside an ELR hydrogel created in a 1:1 composition with two ELR biopolymers via click reaction. Using an oscilloscope, a wave generator and piezoelectrics we measured three Elastin-Like Recombinamers click gels at different PBS concentrations. The objective of the measurement is to understand the propagation of the mechanical waves in hydrogels depending on their composition and frequency of the mechanical waves. This is rather important because mechanical waves may influence the behaviour of a cell.

Resumen.

La producción de recombinadores tipo elastina (ELR en inglés) tiene, como objetivo, la producción de dispositivos nanoestructurados que pudieran ser utilizados para liberación de fármacos y regeneración tisular. El motivo por el cual dichos materiales son tan deseados son sus buenas propiedades mecánicas, biocompatibilidad, biodegradabilidad y su sensibilidad térmica. El objetivo de este trabajo de fin de máster es medir la propagación de ondas mecánicas dentro de un hidrogel creado en una composición 1:1 con dos biopolímeros ELRs mediante una reacción click. Mediante un osciloscopio, un generador de ondas y piezoeléctricos mediremos tres geles click a distintas concentraciones de PBS. El objetivo de dichas mediciones es comprender la propagación de las ondas mecánicas en hidrogeles dependiendo de su composición y de la frecuencia de las ondas mecánicas. Esto es de gran importancia ya que las ondas mecánicas pueden influir en el comportamiento de las células.

1. Introduction.

These last years there has been an increment in the research of polymers that could be applied in the field of biomedicine [2]. The desired characteristics of such materials are biocompatibility, good mechanical properties close to organic tissue, non-aggressive behaviour with cells, degradation without the toxic residues produced from degradation, and easy to handle. The research in components with a well-defined biological topography and the control in the mechanical properties of those are of great interest because of the medical applications like tissue engineering, protein purification, drug delivery between other applications [11].

We can divide the classes of hydrogels into two different types. First, we have the natural hydrogels, these proceed from biomacromolecules like collagen, gelatin, fibrin, hyaluronic acid or silk [8]. These are quite useful because of their mechanical properties. However, they tend to be overspecialized and can not be used in all the fields, also, they have problems with the excessive biodegradability and might produce autoimmune reactions or carry viruses, that is why is needed components with longer longevity and also biodegradable and biocompatible [8]. Other classes of hydrogels used are called synthetic hydrogels. These are, for example, PEG, PLA and PLGA [8]. The main disadvantages of this kind of hydrogel is their poor biocompatibility and biodegradability and, in some cases, can produce inflammations.

One of the most promising polymers are those with the capacity of self-assembly like the elastin-like recombiners (ELR) polymers that we are studying [4, 9]. These materials are protein-based polymers recombinant DNA technologies [5] that allow creating well-defined complex and controlled sequences. The materials are based on the repetition of short peptides considered building blocks of natural elastin [4, 7, 8]. Natural elastin is an insoluble elastic protein that constitutes the main component of flexible tissues where elasticity is of mayor importance like the ligaments, lungs and veins between others. Recently, the availability of recombinant forms of elastin biocompatible with the human body has increased, thus, allowing the creation of a wide range of biomaterial constructs with the properties of elastin's assembly and elasticity.

The term of ELRs highlights the fact that these constructs are oligomeric macromolecules whose composition is strictly defined by genetic engineering and molecular biology. This kind of polymer are produced as recombinant proteins that exhibit monodispersity and high control of amino acid sequences, as well as, that they mimic the basic properties of elastin. ELRs are made of consecutive amino acid sequences from the five-member unit (VPGXG) where X is any natural amino acid except proline or its permutations [4, 7, 8]. ELRs can be tailor-made to form self-assembled systems with controlled

structures as functions. ELRs can include different bioactive sequences such as those for cell adhesion and proliferation or sequences sensitive to enzymes [9]. The thermal sensitivity is characterized by a critical temperature in aqueous solution known as the transition temperature (Tt). This temperature is related to a modification in the organization of the components of the material at a molecular level. If the temperature of the ERL is below of the Tt, then the ERL becomes soluble. This happens because of the configuration of the hydrophobic chains based in the presence of chlorate structures while if the temperature is over the Tt the hydrophobic, clathrate-like hydrated chains of ELRs break, allowing ELRs to fold hydrophobically to form a separate state in which the polymer chains adopt a dynamic, regular, non-random [4] structure. This process is always reversible.

One of the properties of this polymer is the capacity to be genetically encoded. That means a controlled synthesis, precisely to specify molecular weight and amino acid sequences on demand, is possible. Secondly, we can produce ELR from Escherichia coli with great efficiency, then, it can be rapidly purified by exploiting their phase transistor behaviour. As with other natural hydrogels is both biocompatible and biodegradable but, unlike those, it also avoids reactions from the immune system. Because of this ELRs have been used for engineering tissue and drug delivery [6].

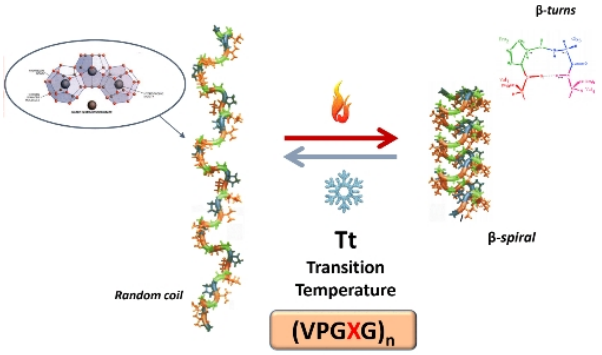

Figure 1: Behaviour of elastin polymers depending on the temperature.

In this work, we will study the behaviour of ELR hydrogels under mechanical forces. We use piezoelectric components connected to an oscilloscope and a wave generator to produce mechanical waves in the hydrogel and will be interpreted as electrical waves in the oscilloscope. using as a reference to the paper [12].

2. Materials and methods.

2.1. Production of ELRs.

The ELRs used in this experiment were constructed using standard genetic-engineering techniques [4, 9]. These hydrogels were produced using cellular systems for genetically engineered protein biosystems in Escherichia coli and purified using several cycles of temperature-dependent reversible precipitations. The purity and molecular weight of the ELR were verified by sodium dodecyl sulfate-polyacrylamide gel electrophoresis (SDS-PAGE) and matrix-assisted laser desorption/ionization time-of-flight (MALDI-TOF) mass spectroscopy using a Voyager STR apparatus from Applied Biosystems [4, 9]. Amino acid composition analysis was also performed. Additional characterization was accomplished using infrared spectroscopy, turbidimetry and nuclear magnetic resonance (NMR) techniques.

In this research, we use two ELRs [4, 9]. The first is called HRGD6 whose structure is MGSSHHHHHHSSGLVPRGSHMESLLP[(VPGIG)2(VPGKG)VPGIG)2] 2AVTGRGDSPASS [(VPGIG)2(VPGKG)(VPGIG)2]6 and the second component is VKV24 whose molecular structure is MESLLP VG VPGVG [VPGKG(VPGVG)5]23 VPGKG VPGVG VPGVG VPGVG VPGV. The physical characteristics of the hydrogels are:

	VKV24	HRGD6
Theoretical pI	11.04	11.10
Molecular weight (g/mol)	60450.91	60649.90

2.2 Chemical modifications of ELR.

In this work, the ELRs were chemically modified by transforming the ε-amine group in the lateral chain in the lysine residue to bear the groups required for the hydrogel formation using click chemistry techniques [1, 4, 9]. The modifications of lysines of the hydrogels were of 80% for the HRGD6 and 60% for the VKV24.

2.3 Modifications in HRGD6 using azides.

A solution of 2-Azidomethil (2,5.Dioxopyrro-lidin-1-YL) Carbonate in anhydrous dimethylformamide (DMF) were added to a solution of the ELR HRGD6 in anhydrous DMF. The resulting mixture was stirred at r.t. 48h. After this time, diethyl ether was added to the mixture to give a white precipitate. The supernatant was removed and the solid was washed with acetone (3 x 15 ml) with centrifugation (12500G, 10 min), dried under reduced pressure, redissolved in cold MQ water (4ºC), dialyzed against MQ water (3 x 25 L) and then the pH of the product was adjusted to 7 and finally, was filtered and lyophilized to yield a white recombinamer (ELR HRGD6-N3).

2.4 Modifications of VKV24 with cyclo.

A solution of (1R, 8S, 9S)-bicyclo[6.1.0]non-4-yn-9-ylmethyl succinimidyl carbonate in anhydrous dimethylformamide (DMF) were added to a solution of the ELR VKV in anhydrous DMF. The resulting mixture was stirred at r.t. 48h. After this time, diethyl ether (30mL) was added to the mixture to give a white precipitate. The supernatant was removed and the solid was washed with acetone (3 x 15 ml) with centrifugation (12500G, 10 min), dried under reduced pressure, redissolved in cold MQ water (4ºC), dialyzed against MQ water (3 x 25 L) and then the product was filtered and

lyophilized to yield a white recombinamer (ELR VKV24-cyclo).

2.5 Fabrication of hydrogels.

The hydrogels were produced combining the HRGD6-azide and VKV24-cyclooctane. First, both components were dissolved in PBS in different proportions inside an Ependorff of 2ml of capacity, then, they were made to be in constant motion overnight in a cold chamber at 4ºC. After that, they are combined in a mould in a 1:1 combination for 30 minutes in the same cold chamber. In the next step, the hydrogels in the mould are exposed to temperatures of 37ºC for 2 hours inside a heater, with this, we have finally produced the hydrogel. Finally, they are preserved in the same fluid in which it was produced inside a Falcon in a fridge at low temperatures. These hydrogels were created with three proportions: 50, 75 and 100 mg/mL of PBS.

2.6. Turbidimetry.

The turbidimetry analysis was realized using a spectrometer (Cary Series UV-Vis, Agilent technologies). The analysis was realized with a wavelength of 350 nm and a range of temperatures between 15ºC to 55ºC with a heating rate of 1.5ºC/min, and a range of measurement of 0.5 ºC. The concentration was, in the measured VKV24 and HRGD6, 50mg/mL in PBS.

2.7 FTIR.

The infrared analysis was realized using a Bruker FTIR spectrometer (Bruker, USA). We collect a 512-scan interferogram in a single beam absorption mode with a resolution of $4cm^{-1}$ for each spectrum in a region between $4000cm^{-1}$ and $600cm^{-1}$. For each sample, several FTIR absorption spectra were collected. These measurements were averaged to obtain the final FTIR absorption spectra. The OPUS (version 4.2) software (MATTSON INSTRUMENT, INC.) performed spectral calculations. The residual water vapour absorption was subtracted from the sample spectra manually.

2.8 NMR.

To analyse the NMR spectra we used a 400MHz Agilent Technologies equip. The measurements were carried out at room temperature (298K). The concentration were 25mg/mL in non-deuterated dimethyl sulfoxide (DMSO-d_6). The chemical shifts (δ) are given in ppm. In order to measure the components of the ELR we use Proton nuclear magnetic resonance.

2.9 Process of measurement.

For the measurements, we use an oscilloscope (KEYSHIGHT DSOX1202A), a wave generator (GW InSTEK AFG-3021) and a pair of piezoelectrics (PAC3CKW, Thorlabs). One of the piezoelectrics is connected to both the wave generator and one of the channels of the oscillator while the other is connected to the second channels of the oscilloscope. The mechanical force is applied with the piezoelectric connected to the wave generator. Both piezoelectrics are placed in parallel in a horizontal plane, between them, we place the hydrogel. The piezoelectrics must have been close enough that the hydrogel does not fall. We select several frequencies between 30-2000 Hz, all with a voltage received from the first channel of $10V_{pp}$.

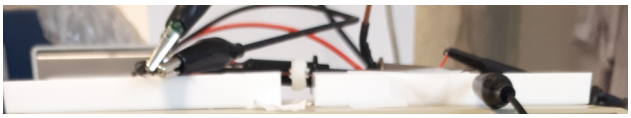

Figure 3: Hydrogel supported by two piezoelectrics connected to the oscilloscope and wave generator.

3. Results and Discussion.

There are two main reasons to study these ELRs, VKV24 and HRGD6. First, HRGD6 is used because of the cellular adhesion sequence RGD that it contain lysines. Second, VKV24 contains a high number of lysines. Thanks to the lysines, they can be chemically modified to form a chemical hydrogel via click reaction. Thanks to this reaction, the hydrogel obtained has higher elasticity and elastic modulus [4, 9]. The reason this happens is because of the VKV24 work as a cross-linker [4, 9] for the HRGD6. Second, the cyclooctane and azide contained in both ELR are required to produce the already mentioned click reactions this is because the alkyne provides a favourable reaction to click reactions.

3.1 Turbidimetry.

In the measurement we could find the Tt of the HRGD6 and VKV24 dissolved in PBS, the temperatures are 28.02ºC and 38.02ºC respectively. We can see that the Tt for the VHV24 is similar to the corporal temperature and the Tt of HRGD6 is almost 10ºC lower.

3.2 Infrared radiation.

In figure 4, the modified VKV24 does not show any significative change in the infrared spectrum compared with the hydrogel without modifications. This could happen because the infrared radiation can not detect the cyclooctane additions. This could mean that the emission is in the same frame as other proteins that VKV24 posses.

In figure 5, comparing the modified and unmodified HRGD6, we see a peak in the latter at $2100cm^{-1}$. This peak, looking in an infrared table [7] correspond to azide, whose peak can be detected between $2160cm^{-1}$ and $2095cm^{-1}$. This result proves that the FTIR can detect quantitatively the modifications produced by azide in the HRGD6.

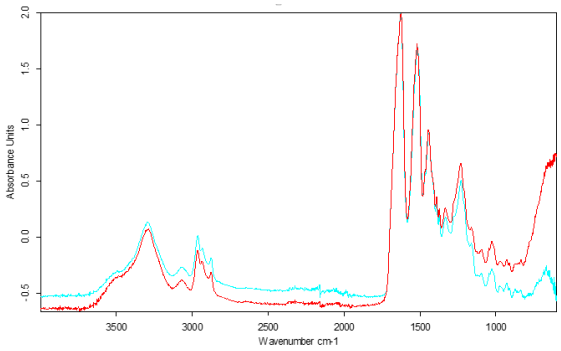

Figure 4: Infrared emission of VKV24 before and after applying the cycles. The blue curve is the infrared emission of VKV24 without applying cycles and the red is the spectra after applying cycles.

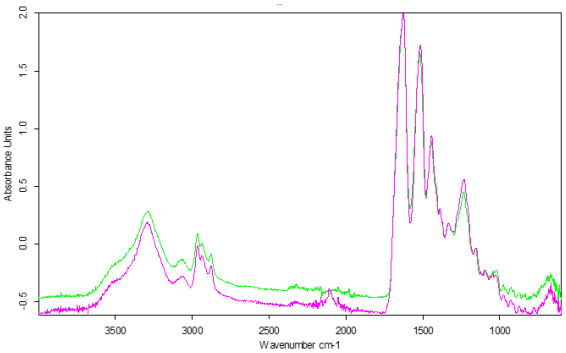

Figure 5: Infrared emission of HRGD6 with and without azides. The green curve is the HRGD6 without azides and the purple is the emission after applying azides.

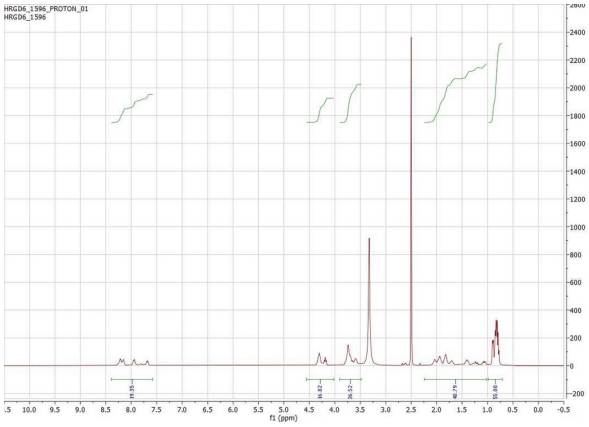

Figure 6: NMR before applying azides to HRGD6.

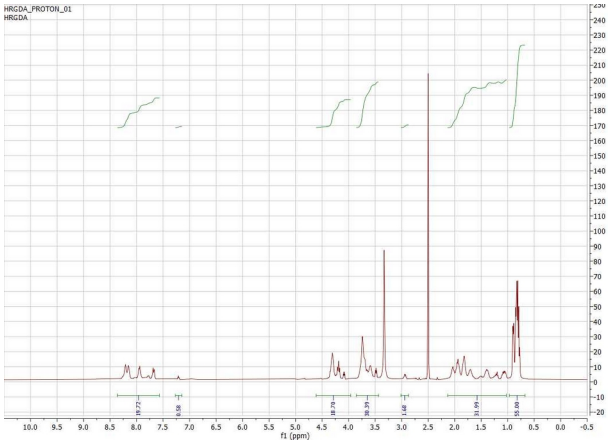

Figure 7: NMR after applying azides to HRGD6.

3.3 NMR.

Thanks to the NMR, we can measure the amount of lysines modified. Seen figure 6 and 7, it is possible to recognize several peaks. The most visible peak can be found near 7ppm. This peak is related to the hydrogen contained in NH inside the azide compound. To calculate the percentage of lysines modified we will take into account three values. First, the value of the integrate in 7ppm. This value should be a reaction to the modification of the lysines in the hydrogel. Second, the peak located between 1 and 0.5 ppm. This peak is the representation of the number of methyls ($-CH_3$) in HRGD6. Finally, knowing the number of methyls ($-CH_3$) that HRGD6 contains, we can calculate the percentage number of modified lysines. Making the calculations we see that the lysines modified are approximately 58%. That means that instead of 19 lysines modified we have approximately 14.

3.4 Mechanical wave propagation.

We measured the three hydrogels at several frequencies and in two waveforms of propagation: sinusoidal mode, for the measurement of the piezoelectrics displacement caused by the mechanical waves travelling across the hydrogel [10] over frequencies, and phase difference between the displacement of the piezoelectrics which causes the mechanical waves and over frequencies. With these values we can draw the graphics that we see in figures 8 and 9. One of the graphs shows the displacements of the piezoelectric in the output signal in the oscilloscope, and the other graph shows the variation of the phase difference for the measured frequencies. The equation to turn the voltages into piezoelectrics displacement is extracted from the data-sheet of the piezoelectric. The second mode, square mode, was used to understand how the waves propagate through the hydrogel.

To explain the behaviour of the wave propagation in the hydrogel we must look at the sinusoidal wave propagation obtained with the equipment of measurement. We can see the sinusoidal behaviour of the wave propagation between the external force produced by one of the piezoelectrics and the force that reaches the second piezoelectric. The stress produced by the external force is represented by the input voltage of the wave generator while the force that reaches the second piezoelectric is represented by the output voltage. The difference in the times between the peaks of the input and the output voltage in the figure is the time displacement necessary to obtain the phase difference and detected by the oscilloscope. When the frequency increases, the phase difference increases and the maximum voltage (the amplitude of the mechanical waves) detected in the output is lesser.

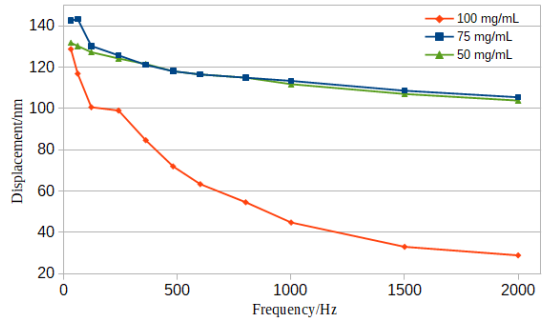

Figure 8: Graph of the output piezoelectric displacement over frequency.

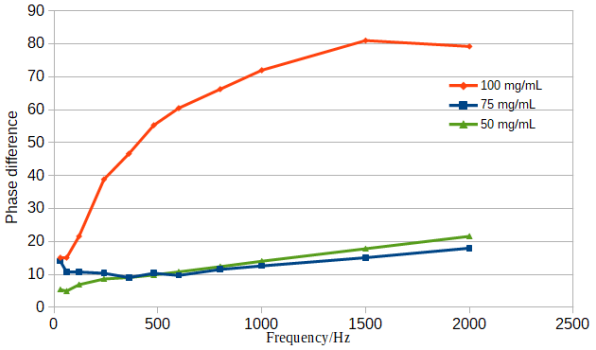

Figure 9: Graphic of the dependency of the phase difference over frequency.

After acquiring the values obtained from the measurement of the propagation of the mechanical waves in the hydrogels (input and output voltage, phase difference and time difference) we can perceive two facts. First, the variation of the mechanical waves of propagation over the frequencies are similar for 50 and 75mg/mL. Second, these variations are greater for 100mg/mL. In the three hydrogels, the output voltage is lower over the frequencies because, at higher frequencies, the interaction in the hydrogel's net is higher, producing an increment in the phase difference. The reduction in the amplitude that are seen in the hydrogels (see figures 8 and 10 to 18) can be also caused by the increment of interactions between the chemical bonds in the hydrogel, producing an increment in the energy loss of the transmission of the mechanical wave.

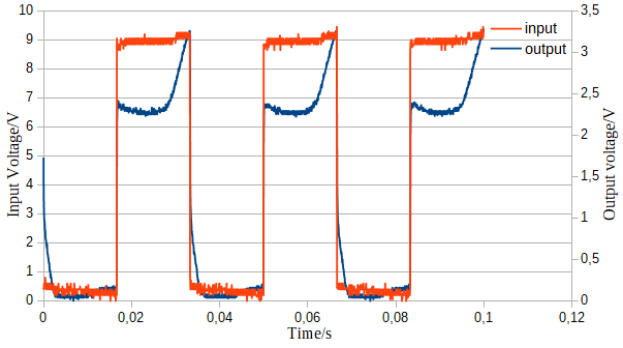

Figure 10: Input and output measurements of the mechanical wave propagation for the ELR of concentration 50mg/mL of PBS at frequencies of 30Hz.

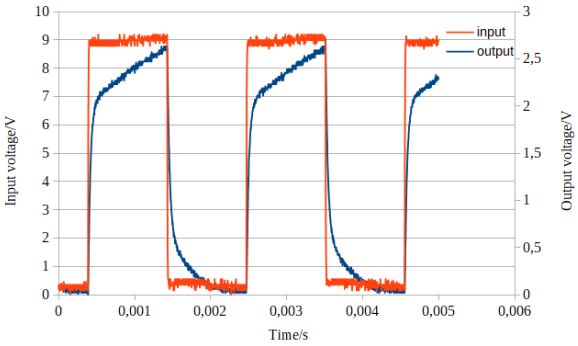

Figure 11: Input and output measurements of the mechanical wave propagation for the ELR of concentration 50mg/mL of PBS at frequencies of 480Hz.

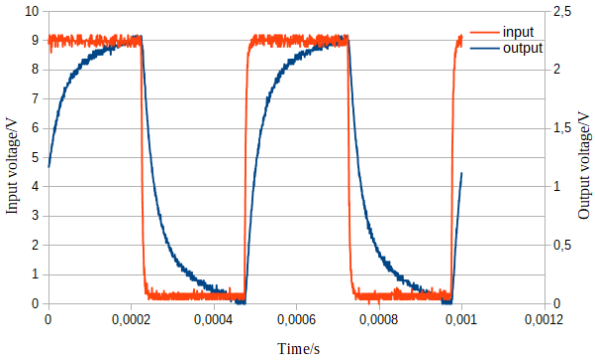

Figure 12: Input and output measurements of the mechanical wave propagation for the ELR of concentration 50mg/mL of PBS at frequencies of 2000Hz.

Looking at the square waves generated by the oscilloscope, we can see how the rheological behaviour of the hydrogel changes over the frequencies. At low frequencies (~30Hz), we can see in the output wave of the oscilloscope in figures 10 and 11 the hydrogels have a visible elastic and viscous mechanical stress. When the frequencies increases (~ 200-2000Hz), we can see in the figures 12 to 15 that, even if the elastic part is present, the viscous part becomes predominant for both the hydrogel of concentration 50 and 75mg/mL of PBS.

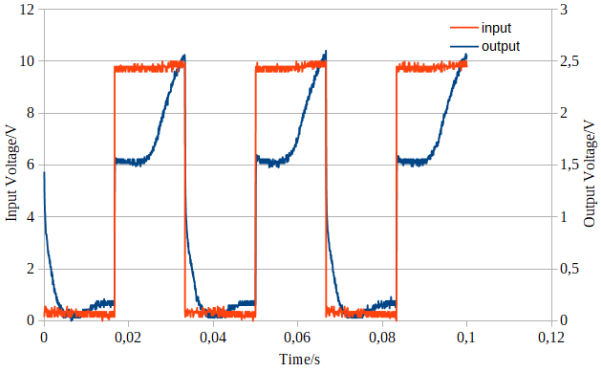

Figure 13: Input and output measurements of the mechanical wave propagation for the ELR of concentration 75mg/mL of PBS at frequencies of 30Hz.

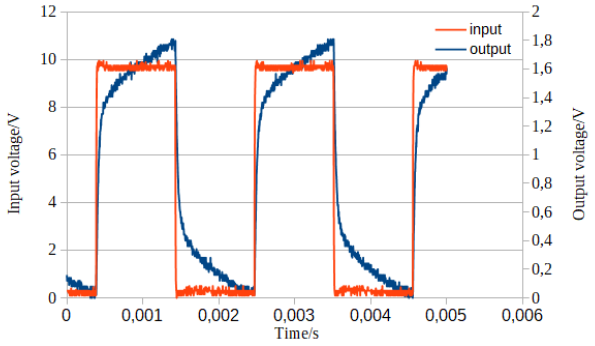

Figure 14:Input and output measurements of the mechanical wave propagation for the ELR of concentration 75mg/mL of PBS at frequencies of 480Hz.

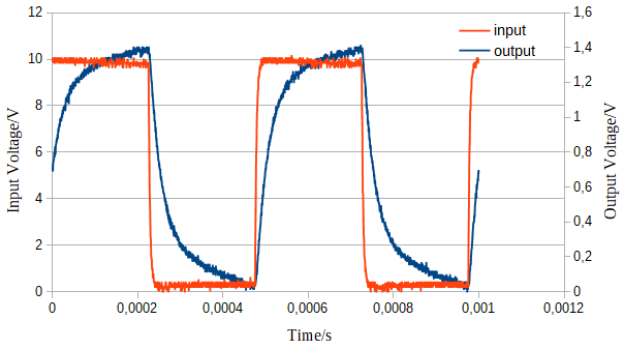

Figure 15: Input and output measurements of the mechanical wave propagation for the ELR of concentration 75mg/mL of PBS at frequencies of 2000Hz

For 100mg/mL, the viscosity is already high at low frequencies (~30Hz). When we increase the frequency of the mechanical waves, we can see how it slowly becomes into a viscous material in figure 17 and, when we reach a frequency of 2000Hz as we can see in figure 18, the hydrogel behaves as if it were completely viscous. Seen the reactions we can assume that the hydrogel behaves like a Kelvin-Voight material [3], considering that the three hydrogels have different elastic and viscous components. These components have, respectively, an elastic and viscous resistance that increases with the frequency. At a certain frequency, the elastic resistance is so high that we can consider that the hydrogel is a viscous material. A good example is the figures 16, 17 and 18. With these reasons, we can assume that at frequencies low enough the viscous resistance will be so low that it will take time until the viscous component of the hydrogel could be appreciated. A good example of this is the figures 10 and 11. The reason of why we think that the hydrogels behave as a Kelvin-Voight material is based on the displacement of the piezoelectric is caused by a force transmitted through the hydrogel and because [3] the stress of the hydrogel in this system is equal to the stress of an elastic system that is constant over time and a viscous system that increases over time. Another reason is the characteristic form that all the waves have for all the hydrogels, except for the hydrogel with concentrations of 100mg/mL of PBS at frequencies higher than 2000Hz because in that case, it behaves as a viscous material.

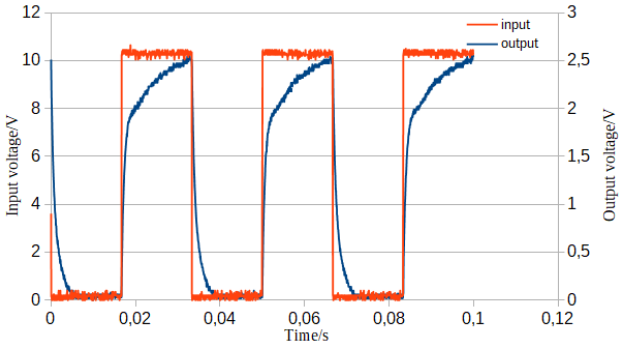

Figure 16: Input and output measurements of the mechanical wave propagation for the ELR of concentration 100mg/mL of PBS at frequencies of 30Hz.

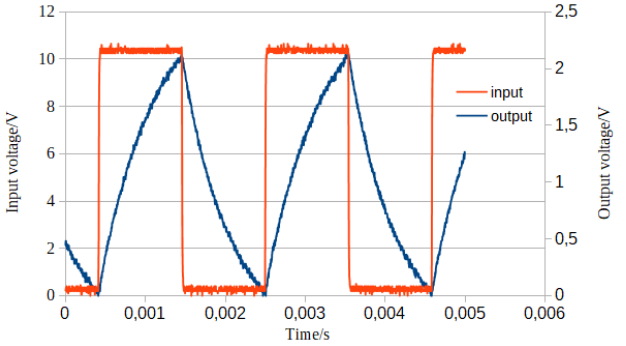

Figure 17: Input and output measurements of the mechanical wave propagation for the ELR of concentration 100mg/mL of PBS at frequencies of 480Hz.

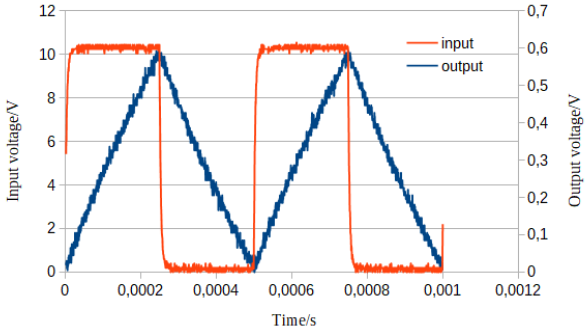

Figure 18: Input and output measurements of the mechanical wave propagation for the ELR of concentration 100mg/mL of PBS at frequencies of 2000Hz.

The difference in the viscoelastic behaviour of the three samples could be caused by the number of chemical bonds in the hydrogels. However, between the ELR with a concentration of 75mg/mL of PBS and the ELR with a concentration of 100mg/mL of PBS the gap in the displacement of the piezoelectric is greater than expected. It could be that the number of chemical bonds skyrockets at the concentration of 100mg/mL. The reason that could produce such change is the reduction of the average pore size of the hydrogel. If this happens, many pores will be so small that they will not let enter PBS in the hydrogel. This way, the hydrogel acquires a more consistent

structure, shorting the path through the bonds when the mechanical waves travel through them.

4. Conclusions.

In this research, we study the wave propagation of mechanical waves with a novel technique to measure the mechanical properties of ELRs hydrogels. In this work, we have used two ELRs, one of them with a cellular adhesion sequence. The results obtained through the measurement of the wave propagation behaves as a Kelvin-Voight viscoelastic. Understanding the rheological and mechanical properties are of great importance. The reason is that understanding these properties will allow us to imitate the extracellular matrix of different tissues. Thanks to this technique we have discovered how waves propagate in the hydrogel. An investigation that could be made in the future is to understand how mechanical waves can affect cellular behaviour.

References.

[1] Hein, C. D., Liu, X. M., and Wang, D. (2008). Click chemistry, a powerful tool for pharmaceutical sciences. *Pharmaceutical research*, *25*(*10*), 2216–2230. https://doi.org/10.1007/s11095-008-9616-1

[2] Ibáñez-Fonseca A., Flora T., Acosta S., Rodríguez-Cabello, J. C. (2019) *Trends in the design and use of elastin-like recombinamers as biomaterials*. Matrix Biology, *84*, 111-126. doi.org/10.1016/j.matbio.2019.07.003.

[3] Özkaya N., Leger D., Goldsheyder D., Nordin M. (2017) *Mechanical Properties of Biological Tissues. In: Fundamentals of Biomechanics*. Springer, Cham. https://doi.org/10.1007/978-3-319-44738-4_15

[4] Quintanilla-Sierra L, García-Arévalo C, Rodriguez-Cabello JC. (2019). Self-assembly in elastin-like recombinamers: a mechanism to mimic natural complexity. *Mater Today Bio*. 2:100007. doi:10.1016/j.mtbio.2019.100007

[5] Rodríguez-Cabello J. C., Girotti A., Ribeiro A., Arias F. J. (2012). Synthesis of genetically engineered protein polymers (recombinamers) as an example of advanced self-assembled smart materials. *Methods Mol Biol*. *811* 17-38. doi:10.1007/978-1-61779-388-2_2.

[6] Rodríguez Cabello, J. C., Testera A., González de Torre, Israel., Santos M., Quintanilla, L., Alonso M. (2014). Elastin-like recombinamer catalyst-free click gels: Characterization of poroelastic and intrinsic viscoelastic properties. *Acta Biomaterialia*, *10 (6)*, 2495-2505. https://doi.org/10.1016/j.actbio.2014.02.006.

[7] Rojo Callejas, F. (n.d.) *Tablas de Espectroscopía Infrarroja*. http://depa.fquim.unam.mx/amyd /archivero/ TablasIR_34338.pdf. Last visit, July 2020.

[8] Song, R., Murphy, M., Li, C., Ting, K., Soo, C., and Zheng, Z. (2018). Current development of biodegradable polymeric materials for biomedical applications. *Drug design, development and therapy*, *12*, 3117–3145.

[9] Testera AM, Girotti A, de Torre IG, et al. (2015) Biocompatible elastin-like click gels: design, synthesis and characterization. *J Mater Sci Mater Med*, *26*, *105* . doi:10.1007/s10856-015-5435-1

[10] Thorlabs. (n.d.) https://www.thorlabs.com/thorproduct.cfm?partnumber=PA3CKW. Last visit, July 2020.

[11] Weil, T. and Barz, M. (2017), From Polymers to Functional Biomaterials. *Macromol. Biosci*., 17: 1700307. doi:10.1002/mabi.201700307

[12] Zareei A, Jiang H, Chittiboyina S, et al. (2020). A lab-on-chip ultrasonic platform for real-time and nondestructive assessment of extracellular matrix stiffness. *Lab Chip*. *20 (4)*, 778-788. doi:10.1039/c9lc00926d.

Supporting information for: Mechanics of Elastin-like Recombinamers hydrogels under mechanical wave pressure.

1. Transfomation of voltage into dispacment and viceversa for the piezoelectric PA3CKW Thorlabs.

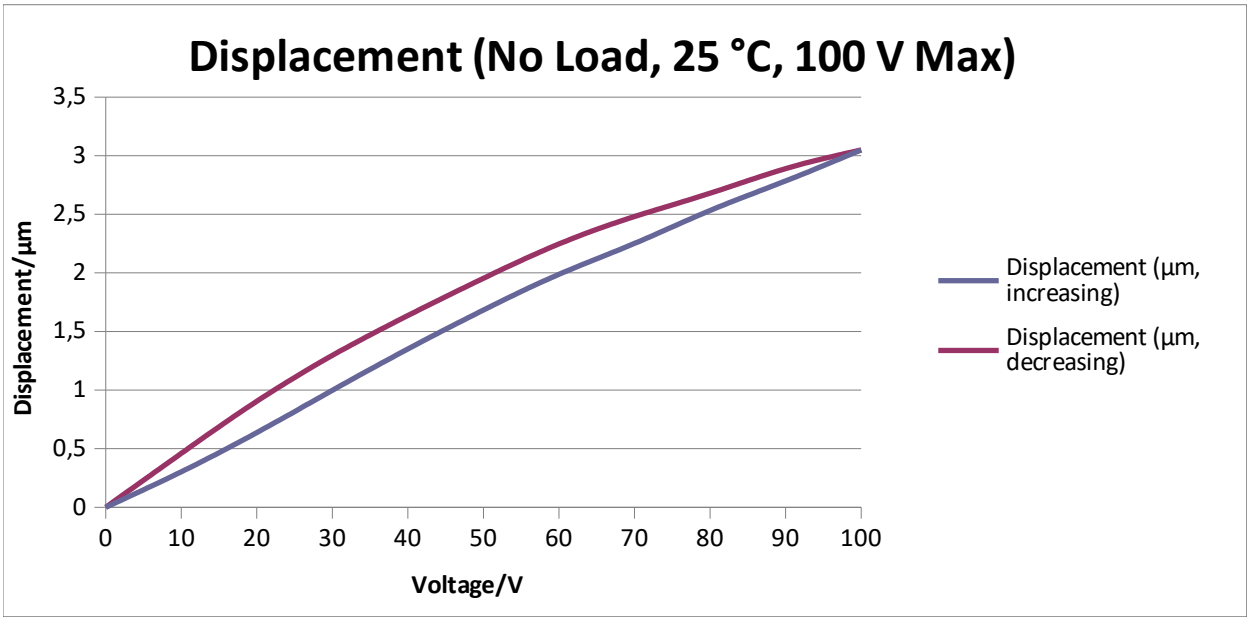

In this graph, there are two curves. One for when the voltage increases the and other when the voltage decreases. The function that represents both curves shall be called $f(V_{up})$ and $f(V_{down})$ recpectivly.

$$f(V_{up}) = -6{,}15157226107225 * 10^{-5} V_{up}^2 + 0{,}037060234988345\, V_{up} - 0{,}039970538461538$$

$$f(V_{down}) = -0{,}00173589102564\, V_{down}^2 + 0{,}04760145710956\, V_{down} + 0{,}008791118881119$$

2. Different values obtained in the viscoelastic measurements

For the hydrogel of concentration 100mg/mL of PBS.

Frequency (Hz)	Voltage (V)	Retard (µs)	Displacement (nm)	Gap º
30	2.81	1400	128.84	15.12
60	2.5	700	116.95	15.12
120	2.09	500	100.7	21.6
240	2.05	450	99.08	38.88
360	1.7	360	84.7	46.66
480	1.4	320	72.03	55.3
600	1.2	280	63.41	60.48
800	1	230	54.66	66.24
1000	0.78	200	44.86	72
1500	0.52	150	33.07	81
2000	0.43	110	28.94	79.2

For the hydrogel of concentration 75mg/mL of PBS.

Frequency (Hz)	Voltage (V)	Retard (µs)	Displacement (nm)	Gap º
30	3.2	1300	142.61	14.04
60	2,97	500	143.34	10.8
120	2.85	250	130.36	10.8
240	2.73	120	125.81	10.37
360	2.61	70	121.21	9.07
480	2.53	60	118.11	10.37
600	2.49	45	116.56	9.72
800	2.45	40	115	11.52
1000	2.41	35	113.43	12.6
1500	2.29	28	108.7	15.12
2000	2.21	25	105.51	18

For the hydrogel of concentration 50 mg/mL of PBS.

Frequency (Hz)	Voltage (V)	Retard (µs)	Displacement (nm)	Gap º
30	2.89	500	131.86	5.4
60	2.85	230	130.36	4.97
120	2.77	160	127.33	6.91
240	2.69	100	124.28	8.64
360	2.62	70	121.59	9.07
480	2.53	57	118.11	9.85
600	2.49	50	116.56	10.8
800	2.45	43	115	12.38
1000	2.37	39	111.86	14.04
1500	2.25	33	107.11	17.82
2000	2.17	30	103.91	21.6

3. HRGD6

```
         10          20          30          40          50          60
MGSSHHHHHH SSGLVPRGSH MESLLPVPGI GVPGIGVPGK GVPGIGVPGI GVPGIGVPGI

         70          80          90         100         110         120
GVPGKGVPGI GVPGIGAVTG RGDSPASSVP GIGVPGIGVP GKGVPGIGVP GIGVPGIGVP

        130         140         150         160         170         180
GIGVPGKGVP GIGVPGIGVP GIGVPGIGVP GKGVPGIGVP GIGVPGIGVP GIGVPGKGVP

        190         200         210         220         230         240
GIGVPGIGAV TGRGDSPASS VPGIGVPGIG VPGKGVPGIG VPGIGVPGIG VPGIGVPGKG

        250         260         270         280         290         300
VPGIGVPGIG VPGIGVPGIG VPGKGVPGIG VPGIGVPGIG VPGIGVPGKG VPGIGVPGIG

        310         320         330         340         350         360
AVTGRGDSPA SSVPGIGVPG IGVPGKGVPG IGVPGIGVPG IGVPGIGVPG KGVPGIGVPG

        370         380         390         400         410         420
IGVPGIGVPG IGVPGKGVPG IGVPGIGVPG IGVPGIGVPG KGVPGIGVPG IGAVTGRGDS

        430         440         450         460         470         480
PASSVPGIGV PGIGVPGKGV PGIGVPGIGV PGIGVPGIGV PGKGVPGIGV PGIGVPGIGV

        490         500         510         520         530         540
PGIGVPGKGV PGIGVPGIGV PGIGVPGIGV PGKGVPGIGV PGIGAVTGRG DSPASSVPGI

        550         560         570         580         590         600
GVPGIGVPGK GVPGIGVPGI GVPGIGVPGI GVPGKGVPGI GVPGIGVPGI GVPGIGVPGK

        610         620         630         640         650         660
GVPGIGVPGI GVPGIGVPGI GVPGKGVPGI GVPGIGAVTG RGDSPASSVP GIGVPGIGVP

        670         680         690
GKGVPGIGVP GIGVPGIGVP GIGVPGKGVP GIGVPGIGV
```

Amino acid composition:

Ala (A)	12	1.7%
Arg (R)	7	1.0%
Asn (N)	0	0.0%
Asp (D)	6	0.9%
Cys (C)	0	0.0%
Gln (Q)	0	0.0%
Glu (E)	1	0.1%
Gly (G)	255	36.5%
His (H)	7	1.0%
Ile (I)	96	13.7%
Leu (L)	3	0.4%
Lys (K)	24	3.4%
Met (M)	2	0.3%
Phe (F)	0	0.0%
Pro (P)	128	18.3%
Ser (S)	24	3.4%
Thr (T)	6	0.9%
Trp (W)	0	0.0%
Tyr (Y)	0	0.0%
Val (V)	128	18.3%
Pyl (O)	0	0.0%

Sec (U) 0 0.0%

(B) 0 0.0%
(Z) 0 0.0%
(X) 0 0.0%

---

4. VKV

```
         10          20          30          40          50          60
MESLLPVGVP GVGVPGKGVP GVGVPGVGVP GVGVPGVGVP GVGVPGKGVP GVGVPGVGVP

         70          80          90         100         110         120
GVGVPGVGVP GVGVPGKGVP GVGVPGVGVP GVGVPGVGVP GVGVPGKGVP GVGVPGVGVP

        130         140         150         160         170         180
GVGVPGVGVP GVGVPGKGVP GVGVPGVGVP GVGVPGVGVP GVGVPGKGVP GVGVPGVGVP

        190         200         210         220         230         240
GVGVPGVGVP GVGVPGKGVP GVGVPGVGVP GVGVPGVGVP GVGVPGKGVP GVGVPGVGVP

        250         260         270         280         290         300
GVGVPGVGVP GVGVPGKGVP GVGVPGVGVP GVGVPGVGVP GVGVPGKGVP GVGVPGVGVP

        310         320         330         340         350         360
GVGVPGVGVP GVGVPGKGVP GVGVPGVGVP GVGVPGVGVP GVGVPGKGVP GVGVPGVGVP

        370         380         390         400         410         420
GVGVPGVGVP GVGVPGKGVP GVGVPGVGVP GVGVPGVGVP GVGVPGKGVP GVGVPGVGVP

        430         440         450         460         470         480
GVGVPGVGVP GVGVPGKGVP GVGVPGVGVP GVGVPGVGVP GVGVPGKGVP GVGVPGVGVP

        490         500         510         520         530         540
GVGVPGVGVP GVGVPGKGVP GVGVPGVGVP GVGVPGVGVP GVGVPGKGVP GVGVPGVGVP

        550         560         570         580         590         600
GVGVPGVGVP GVGVPGKGVP GVGVPGVGVP GVGVPGVGVP GVGVPGKGVP GVGVPGVGVP

        610         620         630         640         650         660
GVGVPGVGVP GVGVPGKGVP GVGVPGVGVP GVGVPGVGVP GVGVPGKGVP GVGVPGVGVP

        670         680         690         700         710         720
GVGVPGVGVP GVGVPGKGVP GVGVPGVGVP GVGVPGVGVP GVGVPGKGVP GVGVPGVGVP


GVGVPGV
```

Amino acid composition:

Ala	(A)	0	0.0%
Arg	(R)	0	0.0%
Asn	(N)	0	0.0%
Asp	(D)	0	0.0%
Cys	(C)	0	0.0%
Gln	(Q)	0	0.0%
Glu	(E)	1	0.1%
Gly	(G)	288	39.6%
His	(H)	0	0.0%
Ile	(I)	0	0.0%
Leu	(L)	2	0.3%
Lys	(K)	24	3.3%
Met	(M)	1	0.1%
Phe	(F)	0	0.0%
Pro	(P)	145	19.9%
Ser	(S)	1	0.1%
Thr	(T)	0	0.0%
Trp	(W)	0	0.0%
Tyr	(Y)	0	0.0%
Val	(V)	265	36.5%
Pyl	(O)	0	0.0%
Sec	(U)	0	0.0%

(B)	0	0.0%
(Z)	0	0.0%
(X)	0	0.0%